Journal of Medicinal Chemistry

pubs.acs.org/jmc

Article

Screening of σ_2 Receptor Ligands and *In Vivo* Evaluation of ^{11}C-Labeled 6,7-Dimethoxy-2-[4-(4-methoxyphenyl)butan-2-yl]-1,2,3,4-tetrahydroisoquinoline for Potential Use as a σ_2 Receptor Brain PET Tracer

Ho Young Kim, Ji Youn Lee, Chia-Ju Hsieh, Aladdin Riad, Nicholas J. Izzo, Susan M. Catalano, Thomas J. A. Graham, and Robert H. Mach*

Cite This: *J. Med. Chem.* 2022, 65, 6261−6272

Read Online

ACCESS | Metrics & More | Article Recommendations | Supporting Information

ABSTRACT: In this study, a panel of 46 compounds containing five different scaffolds known to have high σ_2 receptor affinity were screened. 6,7-Dimethoxy-2-[4-(4-methoxyphenyl)butan-2-yl]-1,2,3,4-tetrahydroisoquinoline [(±)-7] (K_i for σ_1 = 48.4 ± 7.7 nM, and K_i for σ_2 = 0.59 ± 0.02 nM) and its desmethyl analogue, (±)-**8** (K_i for σ_1 = 108 ± 35 nM, and K_i for σ_2 = 4.92 ± 0.59 nM), showed excellent binding affinity and subtype selectivity for σ_2 receptors. *In vitro* cell binding indicated that σ_2 receptor binding of [^{11}C]-(±)-7 and [^{11}C]-(±)-**8** was dependent on TMEM97 protein expression. In PET studies, the peak brain uptake of [^{11}C]-(±)-7 (8.28 ± 2.52%ID/cc) was higher than that of [^{11}C]-(±)-**8** (4.25 ± 0.97%ID/cc) with specific distribution in the cortex and hypothalamus. Brain uptake or tissue binding was selectively inhibited by ligands with different σ_2 receptor binding affinities. The results suggest [^{11}C]-(±)-7 can be used as a PET radiotracer for imaging the function of σ_2 receptors in central nervous system disorders.

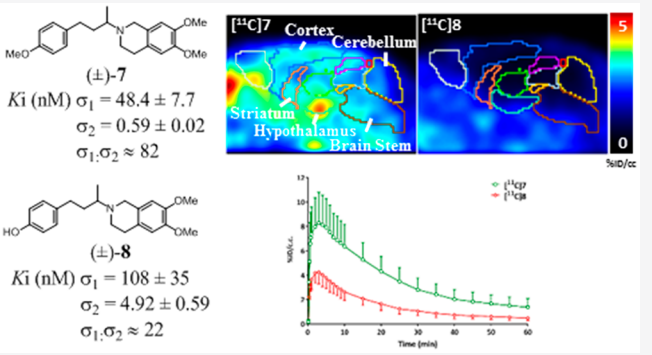

INTRODUCTION

σ receptors were initially considered to be members of the opioid receptor family.[1] However, this receptor was eliminated from the opioid family due to the differential properties of (+)- and (−)-SKF-10047.[2] σ receptors are currently classified into two subtypes, σ_1 and σ_2 receptors. The σ_2 receptor is distinguished from σ_1 receptors by their differences in molecular weight[3,4] (18−21.5 kDa), tissue distribution (brain, liver, and kidney)[5,6] and relative affinity for (+)- and (−)-benzomorphan.[6,7] In 2017, the σ_2 receptor was cloned from calf liver tissue and identified as endoplasmic reticulum (ER)-resident transmembrane protein 97 (TMEM97).[8]

Several ligands for the σ_2 receptor have been developed for an imaging biomarker of cancer because the density of the σ_2 receptor is higher in proliferative cells than in quiescent cells.[9,10] However, research over the past 25 years has demonstrated that the σ_2 receptor is associated with various neurobiological effects, such as intracellular calcium,[11] dopaminergic activity,[12] addiction,[13,14] neuroprotection,[15−17] schizophrenia,[18] anxiety,[19] and depression.[20] Moreover, the complex of σ_2 receptor/TMEM97 with PGRMC1 and the LDL receptor is responsible for the cellular uptake of Aβ42 via its binding to ApoE.[21] According to these studies, the σ_2 receptor is considered a potential therapeutic target for central nervous system (CNS) disorders.

Until now, several selective σ_2 receptor ligands based on different scaffolds have been developed (Figure 1). One of the most promising scaffolds is 6,7-dimethoxy-1,2,3,4-tetrahydroisoquinoline, which was initially identified as part of a program developing dopamine D_3 receptor targeting ligands.[22,23] RHM-4 (**1**) and CM398 (**2**) belong to this class. In cell culture assays, 6,7-dimethoxy-1,2,3,4-tetrahydroisoquinoline derivatives display little cytotoxicity in EMT-6 and MDA-MB-435 cells.[24] [^{18}F]ISO-1, which is the ^{18}F-labeled analogue of RHM-4, is a PET probe for imaging of σ_2 receptor expression in solid tumors[25] and has progressed to clinical trials for imaging primary and metastatic breast cancer. The uptake of these derivatives is highly correlated with σ_2 receptor expression.[26,27] However, the utility of [^{18}F]ISO-1 is limited to peripheral

Received: February 2, 2022
Published: April 11, 2022

https://doi.org/10.1021/acs.jmedchem.2c00191
J. Med. Chem. 2022, 65, 6261−6272

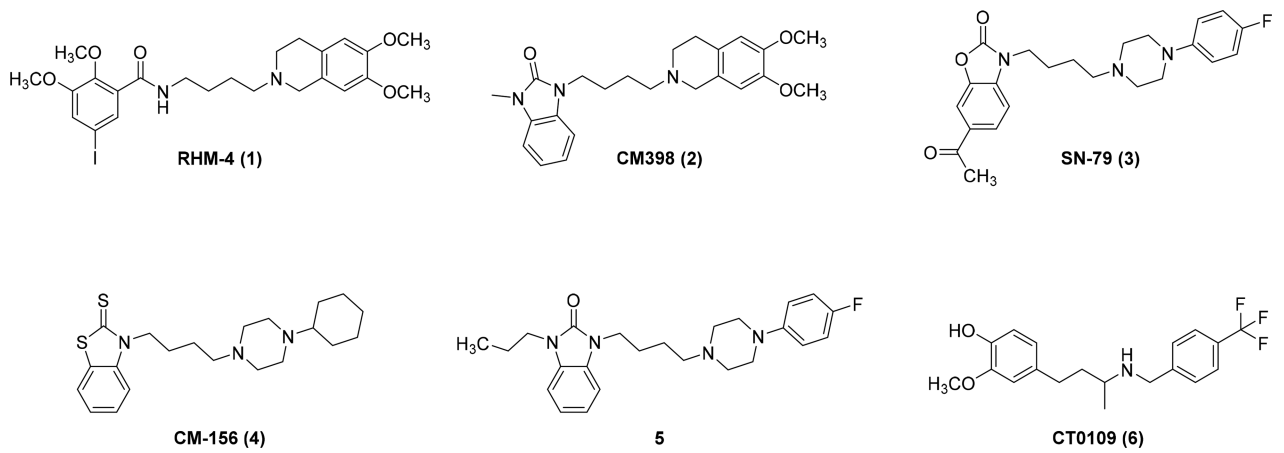

Figure 1. Chemical structures of representative σ_2 receptor ligands with different scaffolds.

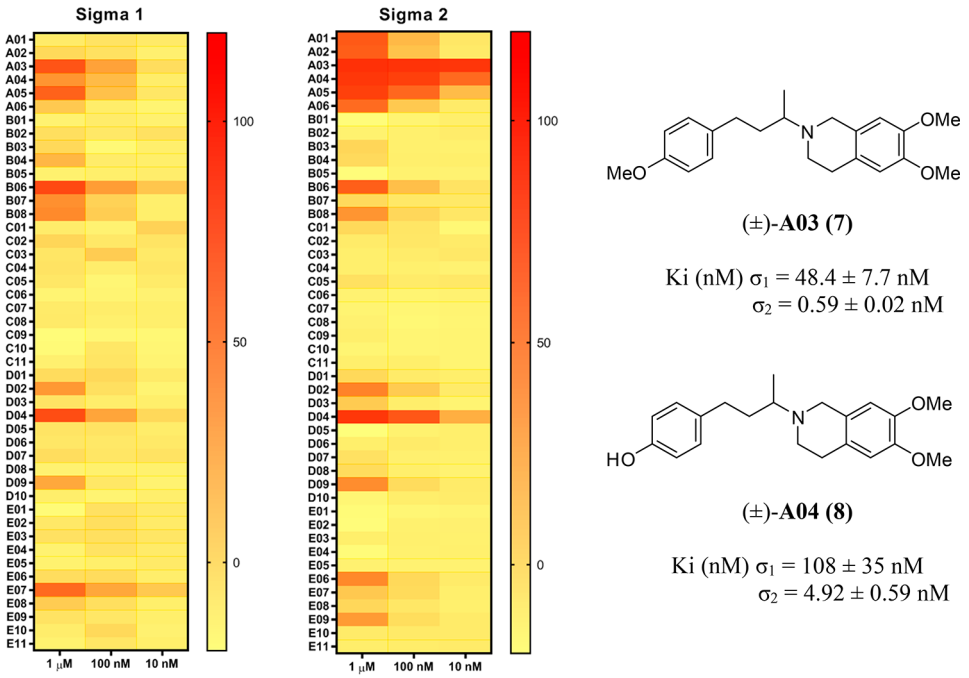

Figure 2. Heat map and the top two compounds for inhibition of σ_1 or σ_2 receptor binding. Binding inhibition was measured at three different concentrations of test compounds against 7.9 nM [^{3}H]-(+)-pentazocine and 0.3 nM [^{125}I]RHM-4. Groups were categorized as (A) 6,7-dimethoxy-1,2,3,4-tetrahydroisoquinoline, (B) benzo[*d*]oxazol-2(3*H*)-one, (C) benzo[*d*]thiazol-2(3*H*)-one or benzo[*d*]thiazol-2(3*H*)-thione, (D) benzo-[*d*]imidazol-2(3*H*)-one, and (E) CT0109 derivatives.

organs due to its low brain uptake. CM398 was more recently developed and showed subnanomolar σ_2 receptor affinity with >1000-fold subtype selectivity.[28] CM398 involved a 3-methyl-1*H*-benzo[*d*]imidazol-2(3H)-one moiety and showed anti-inflammatory analgesic effects; however, a study of its use as a brain PET tracer has not been reported.

Benzo[*d*]oxazol-2(3*H*)-one, benzo[*d*]thiazol-2(3*H*)-one, or benzo[*d*]thiazol-2(3*H*)-thione containing an *N*-arylpiperazine moiety also exhibited high binding affinity for the σ_2 receptor and anti-cocaine activity.[29] Although the compounds were initially developed for the σ_1 receptor,[30] some of the derivatives such as SN79 (**3**) and CM156 (**4**) showed high affinity for the σ_2 receptor and were effective for blocking cocaine-induced convulsions.[31,32] A three-dimensional pharmacophore model for the σ_2 receptor was obtained on the basis of benzo[*d*]-oxazol-2(3*H*)-one derivatives,[33] and new derivatives using this scaffold are still being reported.[34]

In addition to the benzo[*d*]oxazol-2(3*H*)-one scaffold, a series of benzo[*d*]imidazol-2(3*H*)-one-based ligands were synthesized and evaluated for σ_2 receptor binding.[35,36] The benzo[*d*]imidazol-2(3*H*)-one derivative (**5**) showed high binding affinity and selectivity with σ_2 versus σ_1 receptors in *in vitro* binding studies. It showed cocaine-induced anti-convulsion effects in a dose-dependent manner in mice.[36]

Some σ_2 receptor antagonists, such as CT0109 (**6**) and CT1812, can block the binding of the Aβ1−42 oligomer to neurons *in vitro* and showed improvement in cognitive performance in murine models of Alzheimer's disease (AD).[37−39] Although there has been significant effort devoted to the development of specific σ_2 receptor ligands for cancer imaging, there currently is no clinically available PET tracer for measuring the density of σ_2 receptors in the CNS. Recently, σ_2 receptor ligands {e.g., [^{18}F]RM273 or 1-[4-(5,6-dimethoxyi-soindolin-2-yl)butyl]-4-(2-[^{18}F]fluoroethoxy)-1*H*-indole} for

https://doi.org/10.1021/acs.jmedchem.2c00191
J. Med. Chem. 2022, 65, 6261−6272

brain PET have been developed.[40−42] In addition, the σ_2 receptor crystal structure was reported and enabled docking using 490 million virtual molecules.[43] The hit compounds were optimized to have 3−48 nM affinity and 250-fold subtype selectivity. This study demonstrated that it is feasible to identify compounds capable of binding to the σ_2 receptor using *in silico* methods.

In the study presented here, which was initiated prior to the publication of the crystal structure of the σ_2 receptor, an *in silico* search was performed on the MCULE library to identify compounds that are structurally similar to scaffolds known to bind to the σ_2 receptor. The lead compound selected was **1** because of its high affinity and selectivity for the σ_2 receptor and the presence of the basic amine moiety, which is important for σ_2 receptor affinity.[44,45] The goal of this study was to identify new scaffolds and lead compounds that could serve as a σ_2 receptor radiotracer for CNS imaging studies. Two hit compounds were labeled with ^{11}C and evaluated for brain penetration and σ_2 receptor specificity.

RESULTS

***In Vitro* σ_1 and σ_2 Receptor Binding Assay.** An *in silico* similarity search was conducted on a library of 47 million compound, and a panel of 46 compounds having a similarity score of >0.8 for RHM-4 (**1**) were selected. Five different scaffolds were selected for evaluation in this study (Table S1). The 46 selected compounds were screened for σ_1 and σ_2 receptor affinity using 7.9 nM [^{3}H]-(+)-pentazocine (σ_1 receptors) and 0.3 nM [^{125}I]RHM-4 (σ_2 receptors) in a modification of our reported method.[46,47] [^{125}I]RHM-4 was chosen for the σ_2 receptor binding assay because it has a high affinity and excellent selectivity for σ_2 versus σ_1 receptors, which avoids the need to mask σ_1 receptors. In our previous studies, [^{125}I]RHM-4 showed equivalent binding of σ_2 receptors with [^{3}H]DTG.[47,48] The purity of screened compounds was measured prior to the binding assay by LC-MS (Table S2).

The results of the primary screening assay are shown in Figure 2. The highest percent inhibition for the σ_2 receptor was observed with the 6,7-dimethoxy-1,2,3,4-tetrahydroisoquinoline derivatives. (±)-**A03** (**7**) (Figure 2) inhibited 98% of [^{125}I]RHM-4 σ_2 receptor binding and 11% of [^{3}H]-(+)-pentazocine σ_1 receptor binding at a concentration of 100 nM. (±)-**A04** (**8**) (Figure 2), which is the desmethyl analogue of the 4-methoxyphenol moiety in (±)-7, showed the next highest level of inhibition in the σ_2 receptor screening assay (at 100 nM, 34% for the σ_1 receptor and 94% for the σ_2 receptor). The other tested 6,7-dimethoxy-1,2,3,4-tetrahydroisoquinoline derivatives also showed comparatively high percent inhibition for the σ_2 receptors. The other scaffolds that were screened were inactive or showed weak binding to the σ_2 receptor. An exception to this were compounds **B06** and **D04**, which displayed modest binding to both σ_1 and σ_2 receptors.

To confirm the accuracy of the three-point screening assay, the top 21 compounds were selected for full competition curves, and the K_i values for σ_1 receptors and σ_2 receptors are shown in Table S3 and Figure S1. Compound (±)-7 showed the highest binding affinity with a subnanomolar K_i value for the σ_2 receptors (K_i for σ_1 = 48.4 ± 7.7 nM, and K_i for σ_2 = 0.59 ± 0.02 nM) and a selectivity ratio for σ_2 versus σ_1 receptors of 82. Interestingly, the length of the carbon space linker between two aromatic groups was relatively shorter than the distance observed in known σ_2 receptor ligands such as **1**. The featured structure may have benefits in terms of blood−brain barrier (BBB) permeability due to the small polar surface area (PSA) and low molecular weight.[49] Compound (±)-**8** also showed high binding affinity (K_i for σ_1 = 108 ± 35 nM, and K_i for σ_2 = 4.92 ± 0.59 nM) but moderate subtype selectivity (~22-fold). The hydroxy group in **8** can act as the H-bond donor, which may be responsible for the decrease in binding affinity. When the carbon length was reduced by one, the binding affinities in **A01** and **A02** were sharply decreased and the methoxy group seemed not to be involved in the interaction with σ_1 and σ_2 receptors. Introduction of an amide group to give **A05** and **A06** resulted in a further reduction in affinity at both receptors relative to those of 7 and **8**.[50] **D04**, which has an *N*-phenylpiperazine with a butyl linker, showed a comparatively high binding affinity compared to those of the other scaffolds. However, σ_2 receptor subtype selectivity was reduced (for **D04**, K_i for σ_1 = 42.4 ± 3.5 nM and K_i for σ_2 = 19.9 ± 4.7 nM). **B06** and **E07** were intended to be developed as σ_2 receptor ligands but showed moderate binding affinity for σ_1 receptors (for **B06**, K_i for σ_1 = 51.8 ± 6.9 nM and K_i for σ_2 = 179 ± 26 nM; for **E07**, K_i for σ_1 = 68.1 ± 27.2 nM and K_i for σ_2 > 1000 nM). The binding of σ_2 receptors could be more affected by the length of the linker than that of σ_1 receptors.

Compounds (±)-7 and (±)-**8** were initially screened as a racemic mixture. Therefore, the enantiomeric pair of (+)-7 and (−)-7 and the enantiomeric pair of (+)-**8** and (−)-**8** were prepared from (±)-7 and (±)-**8**, respectively, by preparative chiral HPLC. Enantiomeric excess (ee) values of purified enantiomers were measured by analytical HPLC and confirmed to be >99% (chiral HPLC chromatograms in Figure S2). The results in Table 1 indicate that compound (±)-7 had a low eudysmic ratio because the K_i values of both (+)-7 and (−)-7 for σ_2 receptors were very potent (0.63 ± 0.08 and 0.33 ± 0.05 nM, respectively). The binding affinity for σ_1 receptors was very similar to that of (±)-7 [for (+)-7, K_i for σ_1 = 36.8 ± 6.7 nM; for (−)-7, K_i for σ_1 = 39.9 ± 7.1 nM]. Enantiomer (−)-**8** showed higher binding affinity and selectivity for σ_2 receptors than for σ_1 receptors (K_i for σ_1 = 182 ± 85 nM, and K_i for σ_2 = 3.01 ± 0.26 nM) compared to those of (+)-**8** (K_i for σ_1 = 87.6 ± 20.1 nM, and K_i for σ_2 = 10.9 ± 1.2 nM). These results demonstrated the chirality of the methyl group did not significantly affect the binding affinity for σ_1 receptors and σ_2 receptors of (±)-7. On the basis of their receptor binding profiles, (±)-7 and (±)-**8** were labeled with ^{11}C and tested for PET brain uptake and PET imaging studies.

Table 1. *In Vitro* Binding Assay Results for (±)-7 or (±)-8, and Their Enantiomers (+)-7 and (−)-7 or (+)-8 and (−)-8

compound	K_i for σ_1 (nM)	K_i for σ_2 (nM)	selectivity (σ_1/σ_2)
(±)-7	48.4 ± 7.7	0.59 ± 0.02	82
(+)-7	36.8 ± 6.7	0.63 ± 0.08	58
(−)-7	39.9 ± 7.1	0.33 ± 0.05	121
(±)-**8**	108 ± 35	4.92 ± 0.59	22
(+)-**8**	87.6 ± 20.1	10.9 ± 1.21	8
(−)-**8**	182 ± 85	3.01 ± 0.26	60

Synthesis of Standards and Precursors for (±)-7 and (±)-8. Both standards were synthesized efficiently by reductive amination using commercially available reagents (Scheme 1A). The reaction was performed in dichloroethane, and the yield

https://doi.org/10.1021/acs.jmedchem.2c00191
J. Med. Chem. 2022, 65, 6261−6272

Scheme 1. Synthesis of (A) Standards and (B) Precursors[a]

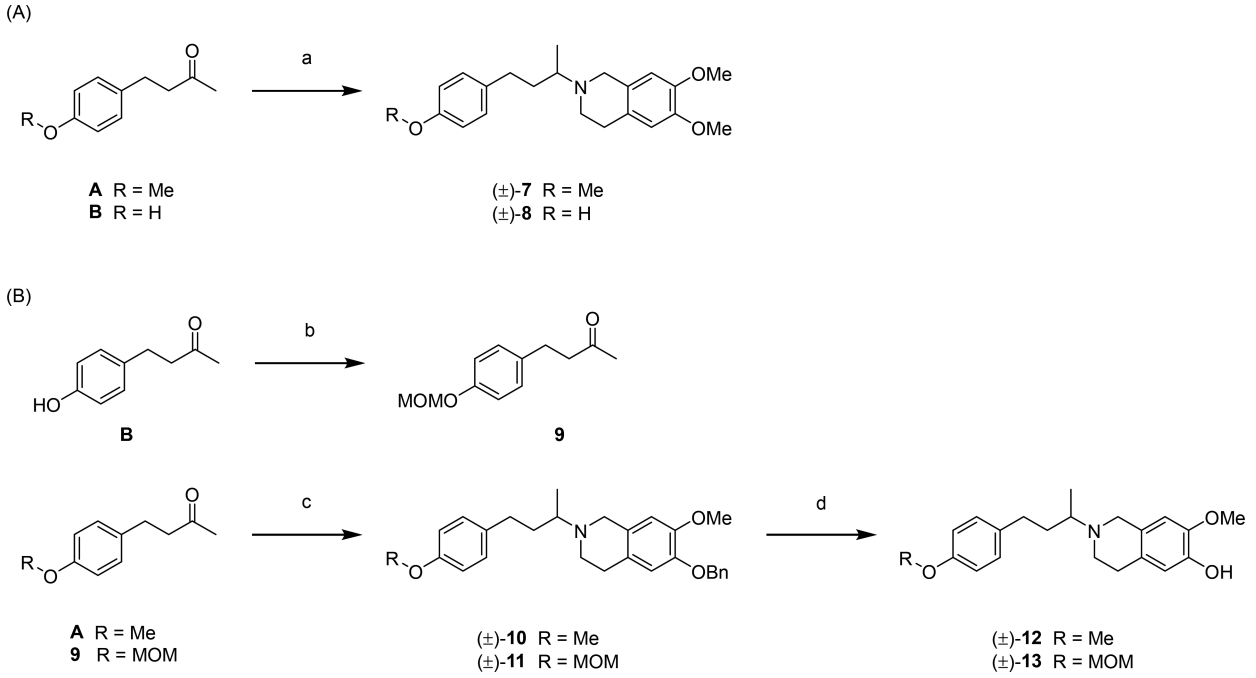

[a]Reagents and conditions: (a) 6,7-dimethoxy-1,2,3,4-tetrahydroisoquinoline, $NaB(OAc)_3$, CH_2Cl_2, room temperature, 24 h; (b) MOMCl, DIPEA, CH_2Cl_2, 0 °C, 3 h; (c) 6-(benzyloxy)-7-methoxy-1,2,3,4-tetrahydroisoquinoline, $NaB(OAc)_3$, dichloroethane, room temperature, 24 h; (d) Pd/C, H_2, MeOH, room temperature, 16 h.

Scheme 2. Radiosynthesis of (A) [^{11}C]-(±)-7 and (B) [^{11}C]-(±)-8[a]

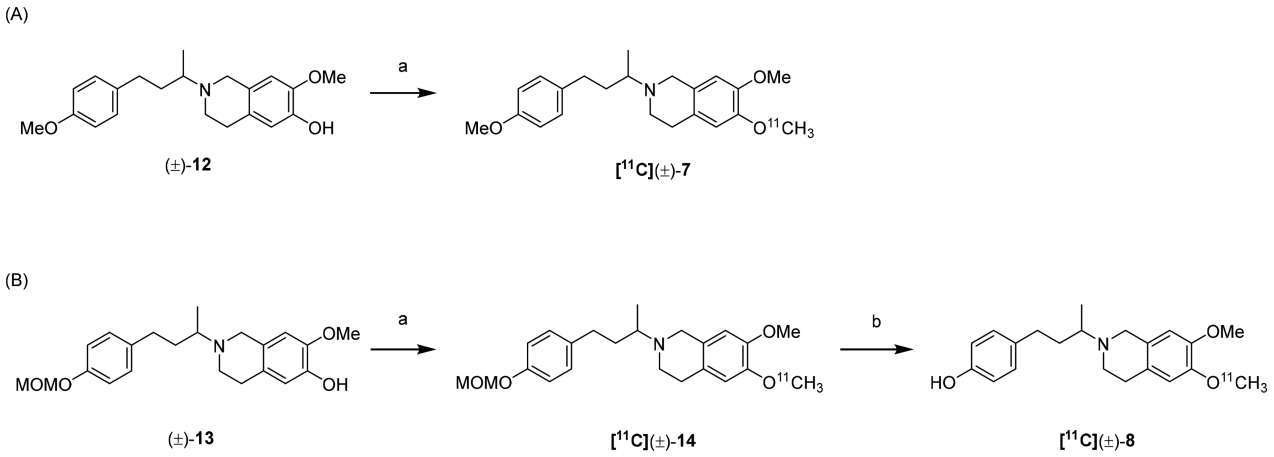

[a]Reagents and conditions: (a) [^{11}C]CH_3I, 5 N NaOH, DMF, 70 °C, 5 min; (b) 2 N HCl, 80 °C, 5 min.

was 25−27%. The solvent was changed to dichloromethane to increase solubility, which resulted in an increased yield (~44%). ^{11}C labeling was performed on the 6,7-dimethoxytetrahydroisoquinoline ring system because this fragment is required for high σ_2 receptor affinity for both **7** and **8**, and the same position can be labeled for comparison of the *in vivo* data. The synthesis of precursors for the radiolabeling studies is shown in Scheme 1B. 6-(Benzyloxy)-7-methoxy-1,2,3,4-tetrahydroisoquinoline was prepared via the Pomeranz−Fritsh reaction according to the reported method.[51] Precursor (±)-**12** for [^{11}C]-(±)-**7** was synthesized by conjugating 4-(4-methoxyphenyl)butan-2-one with 6-(benzyloxy)-7-methoxy-1,2,3,4-tetrahydroisoquinoline followed by the removal of the benzyl protecting group in (±)-**10** using Pd/C and H_2. (±)-**13**, which is the precursor for [^{11}C]-(±)-**8**, was prepared from MOM-protected substrate **9**, via two steps via the same procedure that was used for (±)-**12**. The wavelength absorption of (±)-**7**, (±)-**8**, (±)-**12**, and (±)-**13** was shown to be highest at 230 and 280 nm and lowest at 254 nm.

Radiosynthesis of [^{11}C]-(±)-7 and [^{11}C]-(±)-8. [^{11}C]-(±)-**7** was prepared by reaction of (±)-**12** with [^{11}C]CH_3I in an automated ^{11}C methylation module (Scheme 2A). The total synthesis time for [^{11}C]-(±)-**7** was 40 min, and the radiochemical yield was measured to be 10.0 ± 4.1% (decay corrected to the start of the synthesis; n = 18) based on captured [^{11}C]CO_2. By analytical HPLC, the radiochemical purity was >95% and no significant byproducts were detected. The molar activity was 352 ± 165 GBq/μmol (n = 18), which is suitable for brain receptor imaging. For [^{11}C]-(±)-**8**, (±)-**13** was labeled with [^{11}C]methyl to give [^{11}C]-(±)-**14** followed by

https://doi.org/10.1021/acs.jmedchem.2c00191
J. Med. Chem. 2022, 65, 6261−6272

removal of the MOM group by acid hydrolysis *in situ* (Scheme 2B). It was necessary to reduce the flow rate of the mobile phase from 5 to 3 mL/min to prevent the product from eluting with other ultraviolet (UV)-active impurities. The total synthesis time was 45 min, and the radiochemical yield was 12.9 ± 5.6% (decay corrected to the start of the synthesis; n = 6). The radiochemical purity was >99%, and the molar activity was 255 ± 175 GBq/μmol (n = 6). For *in vivo* studies, MeCN and potassium buffer salts from the HPLC purification of [^{11}C]-(±)-7 and [^{11}C]-(±)-**8** were removed by trapping the radioactivity on a *t*C18 cartridge and elution with ethanol, and the final product was formulated with ethanol/normal saline.

Distribution Coefficient (log $D_{7.4}$). Log $D_{7.4}$ is the measurement of the lipophilicity of the compound and regarded as the important parameter for BBB penetration. The log $D_{7.4}$ values of [^{11}C]-(±)-7 and [^{11}C]-(±)-**8** were measured by the shake-flask method in quintuplicate and determined to be 1.68 ± 0.02 and 1.34 ± 0.00, respectively. [^{11}C]-(±)-7 and [^{11}C]-(±)-**8** with these log $D_{7.4}$ values are well-balanced between solubility and permeability and are good for BBB penetration (optimal value of ∼2).[52]

***In Vitro* Cell Binding Assays.** To confirm the specificity of binding of the ^{11}C-labeled probes to the σ_2 receptors (i.e., σ_2R/TMEM97), cell binding of [^{11}C]-(±)-7 and [^{11}C]-(±)-**8** was performed in control, PGRMC1 knockout (KO), TMEM97 KO, and double KO (DKO) HeLa cells (Figure 3). The

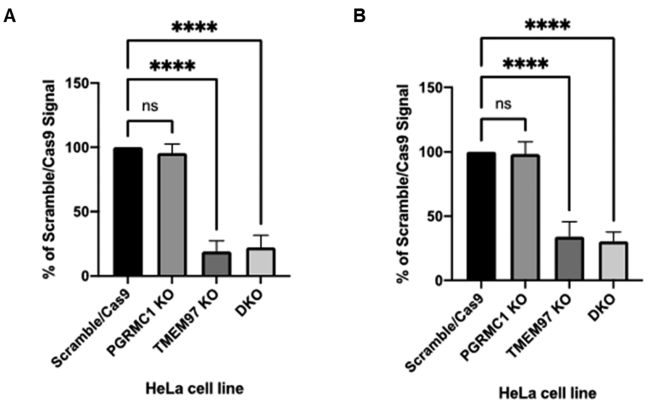

Figure 3. Cell binding studies of 10 nM (A) [^{11}C]-(±)-7 and (B) [^{11}C]-(±)-**8** with four different cell lines: control (scramable/Cas9), PGRMC1 KO, TMEM97 KO, and double KO (DKO). Nonspecific binding was determined by treatment with 10 μM RHM-4. Data represent means ± the standard deviation (n = 3; ****p < 0.0001).

PGRMC1 protein complex was regarded as σ_2 receptors before being identified as TMEM97 by cloning.[47] To confirm whether PGRMC1 or TMEM97 is responsible for the binding, KO cells were prepared by CRISPR technology. [^{11}C]-(±)-7 showed almost the same level of binding in control and PGRMC1 KO HeLa cells. However, the binding was completely eliminated in TMEM97 and double KO HeLa cells. The binding pattern of [^{11}C]-(±)-**8** was similar to that of [^{11}C]-(±)-7; however, the binding level was somewhat higher than that of [^{11}C]-(±)-7 in the TMEM97 KO or DKO cells. The results demonstrate that the binding of [^{11}C]-(±)-7 and [^{11}C]-(±)-**8** with the σ_2 receptor is highly dependent on TMEM97 protein.

***In Vivo* Brain PET Study of the σ_2 Receptor.** PET imaging studies were conducted in C57BL/6J mice to evaluate the brain uptake of [^{11}C]-(±)-7 and [^{11}C]-(±)-**8**. The PET images of [^{11}C]-(±)-7 and [^{11}C]-(±)-**8** at 20−35 min are shown in Figure 4A. [^{11}C]-(±)-7 was widely distributed in the brain, showing high uptake in the cerebral cortex and hypothalamus. The distribution was compared with that of recently reported promising brain-penetrant σ_2 receptor ligands and found similar patterns with a more distinct uptake in cortex.[40,41] On the contrary, [^{11}C]-(±)-**8** did not show any specific distribution in the brain. The specific brain uptake of [^{11}C]-(±)-7 was due to the higher binding affinity and lipophilicity compared to those of [^{11}C]-(±)-**8**, which has a hydroxyl group as opposed to a methoxy moiety in [^{11}C]-(±)-7. The effects on binding affinity and lipophilicity can be better explained by the time−activity curves (TACs). For TACs in Figure 4B, [^{11}C]-(±)-7 showed a high peak uptake in whole brain (8.28 ± 2.52%ID/cc) at 3 min whereas the peak uptake of [^{11}C]-(±)-**8** was lower, 4.25 ± 0.97%ID/cc at 3 min, which indicates [^{11}C]-7 can cross the BBB better than [^{11}C]-(±)-**8** due to the higher lipophilicity. To compare the rate of washout from brain, the TACs were normalized to the peak value of each radiotracer (Figure 4B). The rate of washout of [^{11}C]-(±)-7 was much slower than that of [^{11}C]-(±)-**8**, which is consistent with its higher σ_2 receptor affinity, which leads to a slower rate of dissociation from the receptor. On the basis of these results, we determined that [^{11}C]-(±)-7 was a suitable candidate for σ_2 receptor brain PET imaging.

To investigate the specificity of [^{11}C]-(±)-7 for the σ_2 receptor, PET studies were performed with several blocking agents (1 mg/kg iv, 10 min prior to radiotracer administration): haloperidol (K_i for σ_1 = 1.5 nM, and K_i for σ_2 = 24.2 nM)[53] for σ_1 receptor binding, siramesine (K_i for σ_1 = 12.6 nM, and K_i for σ_2 = 10.5 nM)[54] for σ_2 receptor binding, and (±)-7 for nonspecific binding (Figure 5A). TACs of each group were obtained (Figure 5B). Pretreatment with (±)-7 resulted in a dramatic decrease in the uptake of [^{11}C]-(±)-7 in brain (Figure 5); there was a 40.3% reduction in [^{11}C]-(±)-7 uptake at 20−35 min post-iv injection. However, the uptake of [^{11}C]-(±)-7 was not inhibited by haloperidol (2.6% reduction of tracer uptake at 20−35 min) whereas siramesine inhibited tracer uptake by 21% at the same time point. The different percent blocking in the brain was consistent with different K_i values of ligands for blocking studies. The partial blockade of [^{11}C]-(±)-7 uptake by siramesine may be due to its lower σ_2 receptor affinity or lower brain uptake. The whole body PET uptake also showed high uptake in the liver, which is an organ having a high density of the σ_2 receptor.

Tissue Binding Study in Cortex and Thalamus Homogenates. To further investigate the σ_2 receptor specificity of [^{11}C]-(±)-7, radioligand binding studies were conducted in cortex and thalamus tissue homogenates in the absence and presence of four different blocking agents at 10 nM: (±)-7, haloperidol, siramesine, and (+)-pentazocine (Figure 6). When (±)-7 was used as a blocking agent, there was an ∼90% reduction in the binding of [^{11}C]-(±)-7 in both cortex and thalamus homogenates. A similar result was observed with the σ_2 receptor ligand siramesine. However, haloperidol, which did not inhibit the uptake of [^{11}C]-(±)-7 in PET imaging, resulted in a nonsignificant reduction in the binding of [^{11}C]-(±)-7 to cortex or thalamus homogenates. The lower level of inhibition of radiotracer uptake by haloperidol is likely due to its relatively lower σ_2 receptor binding affinity. (+)-Pentazocine, which is a σ_1 selective ligand, did not inhibit [^{11}C]-(±)-7 binding, and the binding level was similar to the total binding level. On the basis of these results,

https://doi.org/10.1021/acs.jmedchem.2c00191
J. Med. Chem. 2022, 65, 6261−6272

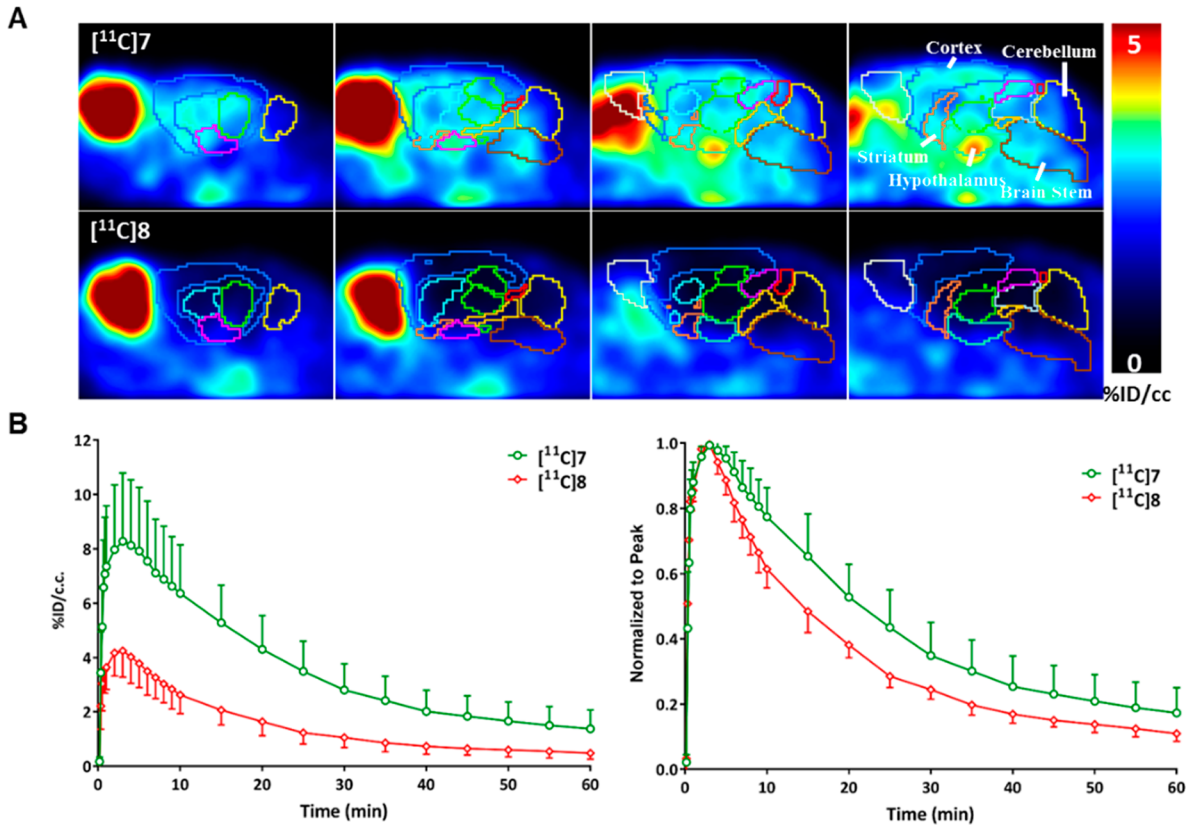

Figure 4. (A) Brain PET images and (B) time–activity (TACs) of [^{11}C]-(±)-7 and [^{11}C]-(±)-**8** in female C57BL/6J mice. The images were obtained 20–35 min after injection, and the TAC was obtained by quantification of the uptake in whole brain. The uptake was normalized to peak to evaluate brain retention of [^{11}C]-(±)-7 and [^{11}C]-(±)-**8** by σ_2 receptor binding.

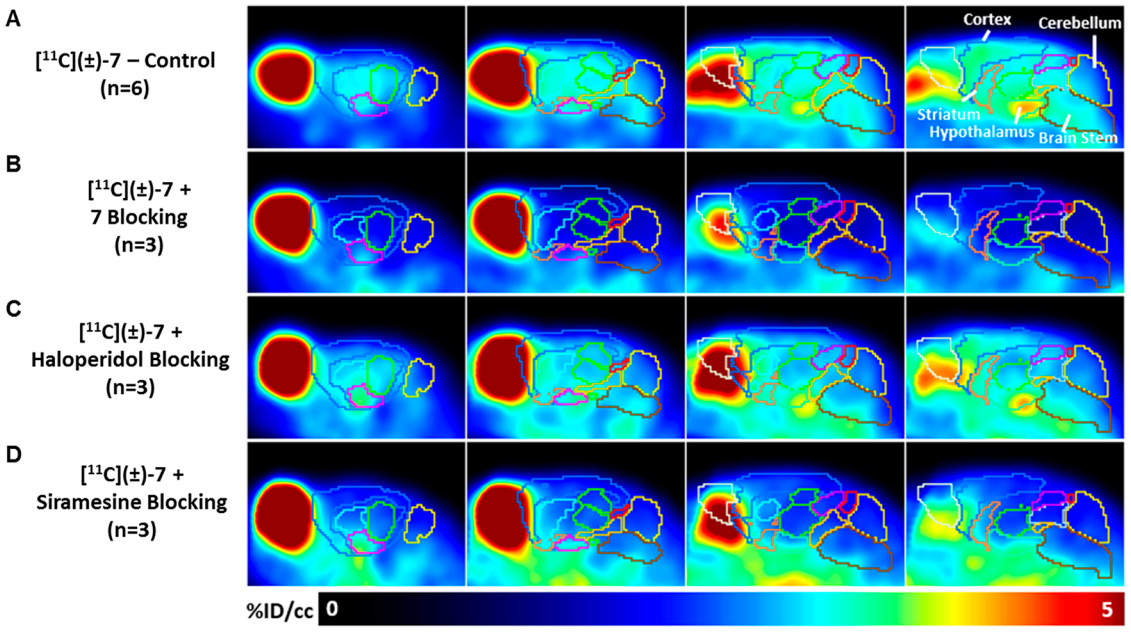

Figure 5. Brain PET images of [^{11}C]-(±)-7 and TACs in control female C57BL/6J mice or mice treated with blocking agents. The images were merged at 20–35 min for (A) control, (B) nonradioactive (±)-7 blocking, (C) haloperidol blocking, and (D) siramesine blocking. The blocking agents (1 mg/kg) were treated 10 min prior to [^{11}C]-(±)-7 injection.

[^{11}C]-(±)-7 has a high selectivity for the σ_2 receptor in the brain.

Metabolite Study. Brain and plasma metabolites were analyzed 30 min after radiotracer injection to determine if radiolabeled metabolites of [^{11}C]-(±)-7 enter the brain or reflect brain PET images (Figure S6). Samples were prepared by extracting brain homogenates or plasma with ethanol. The extraction efficiencies of brain and plasma sample were 79 ±

https://doi.org/10.1021/acs.jmedchem.2c00191
J. Med. Chem. 2022, 65, 6261–6272

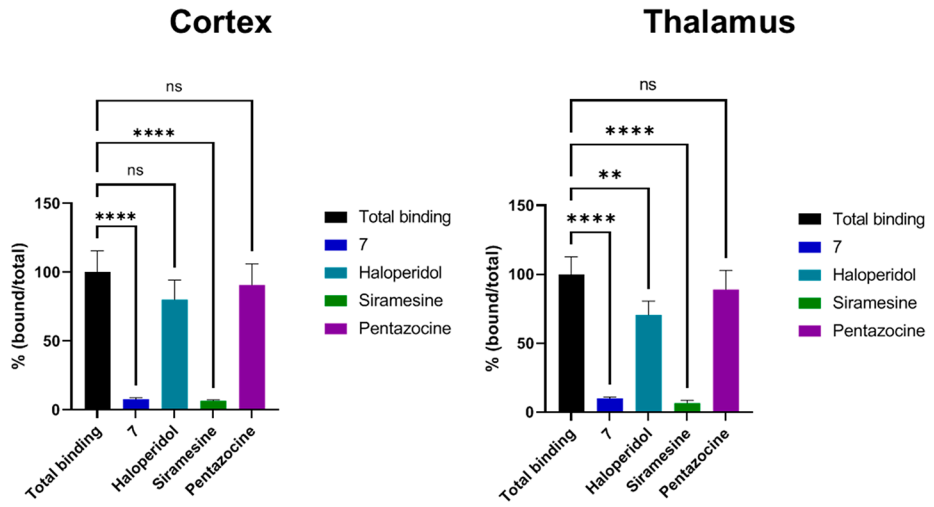

Figure 6. Specific tissue binding of 0.2 nM [^{11}C]-(±)-7 in the presence of four different blocking agents at 10 nM: 7, haloperidol, siramesine, and (+)-pentazocine. Tissue binding was obtained by incubation of cortex or thalamus homogenates for 30 min. Data represent means ± the standard deviation [n = 3; ns indicates no significance ($p > 0.05$), **$p < 0.001$, ***$p < 0.0005$, and ****$p < 0.0001$].

10% and 39 ± 6%, respectively (n = 4). In brain homogenates, 96.6 ± 0.9% of radioactivity was parent compound [i.e., [^{11}C]-(±)-7]; there was a small amount of radioactivity in brain (3.3 ± 1.0%) present as a hydrophilic metabolite. In contrast, 12.5 ± 2.9% of radioactivity in the plasma was parent compound whereas most plasma radioactivity was in the form of polar metabolites (87.5 ± 2.9%). These results indicate that the metabolism of [^{11}C]-(±)-7 is suitable for brain imaging studies because the PET signal from brain is from the parent compound, [^{11}C]-(±)-7.

DISCUSSION

The σ_2 receptor is rapidly becoming an important protein in cell biology. Early studies in our lab identified it as a receptor-based biomarker for imaging cell proliferation in breast cancer cells.[9,10,44] More recent studies have revealed that compounds that function as "σ_2 antagonists" block the uptake of Aβ oligomers by neurons, and CT1812 is currently being evaluated as a disease-modifying drug for treating AD.[37−39,55] Therefore, there is a need to develop radiotracers that are capable of imaging the receptor *in vivo* with the functional imaging technique, PET. Although [^{18}F]ISO-1 has shown promise in clinical imaging studies in breast cancer patients, the low brain uptake of this radiotracer indicates that it is not suitable for CNS imaging studies. During the course of this study, two papers were published reporting σ_2 receptor radiotracers that show good brain uptake and σ_2 receptor binding properties.[40,41]

The goal of this study was to conduct a similarity search on a σ_2 selective radioligand developed in our lab as a means of identifying new scaffolds that could serve as lead compounds for PET radiotracer development. This method involved searching a library of 47 million compounds available from MCULE. This search engine is very simple to use and does not require a working knowledge of advanced computational chemistry methods. A select group of scaffolds were chosen for screening in a three-point high-throughput screening assay, and a subset of 21 compounds were selected for full evaluation for *in vitro* binding assays. The main observation from this study is that it is possible to identify potent compounds for a target receptor using a simple similarity search of a commercially available compound library. In addition, our results indicated that the three-point high-throughput screening assay was accurate in identifying lead compounds for more detailed *in vitro* characterization. This similarity search identified two compounds, (±)-7 and (±)-**8**, that had excellent σ_2 receptor affinities and good subtype selectivities for σ_2 versus σ_1 receptors. Both (±)-7 and (±)-**8** have an asymmetric center and resolution of each to their corresponding enantiomeric pairs indicated that (±)-7 has a low eudysmic ratio whereas (−)-**8** had a higher σ_2 receptor affinity and better selectivity versus σ_1 receptors than (+)-**8**. The racemic mixture of both compounds was radiolabeled with ^{11}C, and [^{11}C]-(±)-7 appeared to have *in vivo* properties that were better than those of [^{11}C]-(±)-**8**. The initial imaging studies were conducted on the racemic mixture of (±)-7 and (±)-**8**. Further studies are being conducted on [^{11}C]-(+)-7 and [^{11}C]-(−)-7 to determine if the stereochemistry factors into the *in vivo* behavior of this compound.

The recent publication of the crystal structure of the σ_2 receptor[43] indicates that it is now possible to conduct protein-based *in silico* screening of compound libraries as opposed to the ligand-based screen described in this report. The high-throughput screening method described above indicates that it will be possible to screen large libraries of "*in silico* hits" using more sophisticated, protein-based ultra-high-throughput screening methods previously used by our group in identifying small molecules that bind to α-synuclein fibrils.[56] These studies are currently ongoing in our lab.

CONCLUSION

There is a growing need for a radiotracer capable of imaging σ_2 receptors in the CNS. Among the panel of compounds screened in this study, compound (±)-7 showed subnanomolar binding affinity and a subtype selectivity for σ_2 versus σ_1 receptors. [^{11}C]-(±)-7 was successfully synthesized and showed high brain uptake and a slow rate of washout from brain. The high uptake and regional distribution suggested [^{11}C]-(±)-7 is consistent with the regional density of σ_2 receptors in the brain. The specificity of [^{11}C]-(±)-7 for σ_2 receptors was evaluated by blocking studies with blocking agents that have different σ_2 receptor binding affinity. Tissue

https://doi.org/10.1021/acs.jmedchem.2c00191
J. Med. Chem. 2022, 65, 6261−6272

homogenate binding confirmed the specific σ_2 receptor binding in the brain. Moreover, the metabolism profile in the brain and the plasma was suitable for brain receptor PET imaging. However, low uptake in hippocampus and cerebellum remains unclear, a result that was also observed in previous studies. Nevertheless, [^{11}C]-(±)-**7** was very potent and showed specific binding to the σ_2 receptor in brain. These results demonstrated [^{11}C]-(±)-**7** has potential for studying the role of the σ_2 receptor in CNS disorders.

EXPERIMENTAL SECTION

General. A total of 46 compounds for screening were identified from the core of known σ_2 receptor ligands by similarity searching from the Web site of Mcule, Inc. (https://mcule.com/), and selected by visual inspection. Mcule, Inc., was supplied with compounds from ChemBridge, ChemDiv, Enamine, FCH group, InterBioScreen, Ukrorgsynthez, and VITAS M Chemical Ltd. Before screening, the purity of compounds was checked using a 2695 Alliance LC-MS instrument. The other reagents and solvents were purchased from Sigma-Aldrich (St. Louis, MO) and TCI (Tokyo, Japan) and used as received. Reactions were monitored by thin layer chromatography (TLC) using TLC silica gel 60W $F_{254}S$ plates, and the spots were detected under UV light (254 nm) or developed using ninhydrin. Flash column chromatography was carried out on a Biotage Isolera One instrument with a dual-wavelength UV−visible detector. ^{1}H and ^{13}C NMR spectra were recorded on a Bruker NEO-400 spectrometer (Bruker). Chemical shifts (δ) were recorded in parts per million relative to the deuterated solvent as an internal reference. Mass spectra (m/z) were recorded on a model 2695 Alliance LC-MS instrument (Waters Corp.) using positive electrospray ionization (ESI^+). High-resolution mass spectra (HRMS, m/z) were acquired on a Waters LCT premier mass spectrometer (Waters Corp.). Optical rotations were obtained using a JASCO P-1000 polarimeter. All animal experiments were performed under protocols approved by the University of Pennsylvania Institutional Animal Care and Use Committee.

***In Vitro* Binding Assay.** [^{3}H]-(+)-Pentazocine (7.9 nM, 50 μL, ∼50000 cpm) or [^{125}I]RHM-4 (0.3 nM, 50 μL, ∼200000 cpm) was mixed with three different concentration of tested compounds (10 nM, 100 nM, and 1 μM). Guinea pig brain homogenates (100 μg/100 μL) or rat liver homogenates (15 μg/100 μL) were added to the mixture and incubated at 37 °C at 90 min. The mixture (200 μL) was filtered with a harvester and washed three times using cold washing buffer (10 mM Tris-HCl and 150 mM NaCl) using a harvester. The collected filtrate was mixed with 3 mL of microscint20 and counted at 1 min/well using a β counter. To obtain specific binding affinities, the tested compound was prepared at concentrations ranging from 10^{-5} to 10^{-11} M for σ_1 or from 10^{-5} to 10^{-14} M for σ_2 using assay buffer [50 mM Tris-HCl and 0.1% bovine serum albumin (BSA) (pH 8)] and mixed with [^{3}H]-(+)-pentazocine and guinea pig brain homogenates or [^{125}I]RHM-4 and rat liver homogenates (15 μg/100 μL), respectively. The mixture was incubated at 37 °C for 90 min. [^{3}H]-(+)-Pentazocine- or [^{125}I]RHM-4-bound compounds were filtered with a Whatman CF/C filter that was soaked in 1% polyethylenimine (PEI) in DW, and then the filtrate was washed three times with cold washing buffer. Nonspecific binding was assessed in the presence of 10 μM haloperidol or RHM4. The filtrate was collected and mixed with microscint20 overnight before scintillation counting (MicroBeta^2, PerkinElmer). The result was analyzed using PRISM 8 software.

Chemistry. *Synthesis of 6,7-Dimethoxy-2-[4-(4-methoxyphenyl)butan-2-yl]-1,2,3,4-tetrahydroisoquinoline [(±)-**7**].* In a solution of 4-(4-methoxyphenyl)butan-2-one (2.14 g, 12 mmol) and 6,7-dimethoxy-1,2,3,4-tetrahydroisoquinoline (2.32 g, 12 mmol) in CH_2Cl_2 (30 mL), $NaB(OAc)_3$ (6.36 g, 30 mmol) was added and the reaction mixture was stirred at room temperature for 24 h. When the reaction was completed, the reaction mixture was diluted with CH_2Cl_2 and washed with saturated $NaHCO_3$ and brine. The reaction mixture was dried over anhydrous magnesium sulfate and filtered, and the solvent was removed under reduced pressure. The crude product was purified by flash chromatography on silica gel (2:1:0.01 EtOAc/hexane/7 N NH_3 in MeOH) to afford (±)-**7** (1.88 g, 44% yield) as a slightly light yellow oil: ^{1}H NMR (400 MHz, $CDCl_3$) δ 7.09 (d, J = 8.6 Hz, 2H), 6.80 (d, J = 8.6 Hz, 2H), 6.57 (s, 1H), 6.51 (s, 1H), 3.82 (s, 3H), 3.81 (s, 3H), 3.76 (s, 3H), 3.70 (d, J = 14 Hz, 1H), 3.60 (d, J = 14 Hz, 1H), 2.80−2.73 (m, 4H), 2.69−2.55 (m, 3H), 1.98−1.89 (m, 1H), 1.66−1.57 (m, 1H), 1.08 (d, J = 6.6 Hz, 3H); ^{13}C NMR (100 MHz, $CDCl_3$) δ 157.7, 147.4, 147.2, 134.6, 129.3, 126.6, 113.7, 111.5, 109.6, 58.0, 55.9$_4$, 55.9$_2$, 55.3, 50.6, 45.9, 35.7, 32.1, 29.4, 13.8; ESI-MS calcd for $C_{22}H_{30}NO_3^+$ $[M + H]^+$ m/z 356.5, found m/z 356.5; HRMS (ESI) for $C_{22}H_{30}NO_3^+$ $[M + H]^+$ requires m/z 356.2226, found m/z 356.2217.

*Synthesis of 4-[3-(6,7-Dimethoxy-3,4-dihydroisoquinolin-2(1H)-yl)butyl]phenol [(±)-**8**].* (±)-**8** was synthesized via the same procedure that was used for (±)-**7** and purified by flash chromatography on silica gel (20:1 CH_2Cl_2/7 N NH_3 in MeOH) to afford (±)-**8** (1.55 g, 38% yield) as a white solid: ^{1}H NMR (400 MHz, $CDCl_3$) δ 6.95 (d, J = 8.4 Hz, 2H), 6.60 (d, J = 8.4 Hz, 2H), 6.55 (s, 1H), 6.50 (s, 1H), 3.80 (d, J = 1.5 Hz, 6H), 3.70 (d, J = 14 Hz, 1H), 3.61 (d, J = 14 Hz, 1H), 2.82−2.73 (m, 4H), 2.72−2.59 (m, 2H), 2.54−2.47 (m, 1H), 1.98−1.90 (m, 1H), 1.67−1.58 (m, 1H), 1.08 (d, J = 6.5 Hz, 3H); ^{13}C NMR (100 MHz, $CDCl_3$) δ 154.1, 147.4, 147.2, 133.8, 129.4, 126.9, 126.5, 115.3, 111.5, 109.6, 57.8, 55.9$_3$, 55.8$_9$, 50.1, 46.2, 35.7, 32.1, 29.2, 13.2; ESI-MS calcd for $C_{21}H_{29}NO_3^{2+}$ $[M + 2H]^+$ m/z 343.5, found m/z 343.5; HRMS (ESI) for $C_{21}H_{28}NO_3^+$ $[M + H]^+$ requires m/z 342.2069, found m/z 342.2054.

*Synthesis of 4-[4-(Methoxymethoxy)phenyl]butan-2-one (**9**).* A solution of 4-(4-hydroxyphenyl)butan-2-one (1 g, 6.1 mmol) and DIPEA (1.59 mL, 9.1 mmol) in CH_2Cl_2 (10 mL) and chloromethyl methyl ether was added at 0 °C, and the reaction mixture was stirred at 0 °C for 3 h. When the reaction had reached completion, the mixture was washed using water and brine, dried over $MgSO_4$, filtered, and concentrated *in vacuo*. The residue was purified by flash chromatography on silica gel (4:1 *n*-hexane/ethyl acetate) to afford **9** (1 g, 81% yield) as a colorless oil: ^{1}H NMR (400 MHz, $CDCl_3$) δ 7.08 (d, J = 8.6 Hz, 2H), 6.93 (d, J = 8.6 Hz, 2H), 5.12 (s, 2H), 3.45 (s, 3H), 2.82 (d, J = 7.6 Hz, 2H), 2.70 (d, J = 7.6 Hz, 2H), 2.11 (s, 3H); ^{13}C NMR (100 MHz, $CDCl_3$) δ 208.0, 155.6, 134.4, 129.3, 116.4, 94.6, 55.9, 45.4, 30.1, 28.9; ESI-MS calcd for $C_{12}H_{17}O_3^+$ $[M + H]^+$ m/z 209.3, found m/z 209.3.

*Synthesis of 6-(Benzyloxy)-7-methoxy-2-[4-(4-methoxyphenyl)-butan-2-yl]-1,2,3,4-tetrahydroisoquinoline [(±)-**10**].* (±)-**10** was synthesized using 6-(benzyloxy)-7-methoxy-1,2,3,4-tetrahydroisoquinoline and dichloroethane via the same procedure that was used for (±)-**7** to afford (±)-**10** (400 mg, 25% yield) as a slightly light yellow oil: ^{1}H NMR (400 MHz, $CDCl_3$) δ 7.41 (d, J = 7.2 Hz, 2H), 7.34 (t, J = 7.1 Hz, 2H), 7.28 (d, J = 7.2 Hz, 1H), 7.09 (d, J = 8.6 Hz, 2H), 6.80 (d, J = 8.6 Hz, 2H), 6.61 (s, 1H), 6.54 (s, 1H), 5.08 (s, 2H), 3.82 (s, 3H), 3.77 (s, 3H), 3.71 (d, J = 13 Hz, 1H), 3.61 (d, J = 14 Hz, 1H), 2.76 (br, 4H), 2.68−2.54 (m, 3H), 1.94 (br, 1H), 1.67−1.59 (m, 1H), 1.09 (d, J = 6.4 Hz, 3H); ^{13}C NMR (100 MHz, $CDCl_3$) δ 157.9, 148.1, 146.9, 137.5, 129.5, 128.7, 127.9, 127.5, 114.6, 113.9, 110.5, 71.4, 56.3, 55.5, 46.1, 32.2, 14.0; ESI-MS calcd for $C_{28}H_{35}NO_3^{2+}$ $[M + 2H]^+$ m/z 433.6, found m/z 433.6.

*Synthesis of 6-(Benzyloxy)-7-methoxy-2-{4-[4-(methoxymethoxy)phenyl]butan-2-yl}-1,2,3,4-tetrahydroisoquinoline [(±)-**11**].* (±)-**11** was synthesized using 6-(benzyloxy)-7-methoxy-1,2,3,4-tetrah-droisoquinoline and dichloroethane via the same procedure that was used for (±)-**7** to afford (±)-**11** (180 mg, 27% yield) as a colorless oil: ^{1}H NMR (400 MHz, $CDCl_3$) δ 7.41 (d, J = 7.3 Hz, 2H), 7.33 (t, J = 7.1 Hz, 2H), 7.27 (d, J = 7.3 Hz, 1H), 7.09 (d, J = 8.6 Hz, 2H), 6.93 (d, J = 8.6 Hz, 2H), 6.60 (s, 1H), 6.54 (s, 1H), 5.13 (s, 2H), 5.08 (s, 2H), 3.82 (s, 3H), 3.67 (d, J = 14 Hz, 1H), 3.57 (d, J = 14 Hz, 1H), 3.46 (s, 3H), 2.78−2.70 (m, 4H), 2.68−2.55 (m, 3H), 1.95−1.86 (m, 1H), 1.65−1.55 (m, 1H), 1.06 (d, J = 6.6 Hz, 3H); ^{13}C NMR (100 MHz, $CDCl_3$) δ 155.5, 148.1, 146.8, 137.6, 136.3, 129.6, 128.7, 127.9, 127.5, 127.0, 116.4, 114.7, 110.5, 94.9,

https://doi.org/10.1021/acs.jmedchem.2c00191
J. Med. Chem. 2022, 65, 6261−6272

71.4, 58.1, 56.3, 56.1, 51.0, 46.0, 36.0, 32.4, 29.7, 14.0; ESI-MS calcd for $C_{29}H_{37}NO_4^{2+}$ $[M + 2H]^+$ m/z 463.6, found m/z 463.6.

Synthesis of 7-Methoxy-2-[4-(4-methoxyphenyl)butan-2-yl]-1,2,3,4-tetrahydroisoquinolin-6-ol [(±)-12]. A solution of (±)-**10** (30 mg, 0.07 mmol) and Pd/C (10%, 5 mg) in MeOH (3 mL) was degassed and treated with H_2 gas. The reaction mixture was stirred at room temperature for 4 h and filtered through Celite. The solvent was removed under reduced pressure, and the residue was purified by flash chromatography on silica gel (20:1 CH_2Cl_2/7 N NH_3 in MeOH) to afford (±)-**12** (12 mg, 50% yield) as a white solid: ^{1}H NMR (400 MHz, $CDCl_3$) δ 7.09 (d, J = 8.6 Hz, 2H), 6.80 (d, J = 8.6 Hz, 2H), 6.64 (s, 1H), 6.48 (s, 1H), 3.81 (s, 3H), 3.77 (s, 3H), 3.77−3.72 (m, 2H), 2.85 (br, 4H), 2.71−2.54 (m, 3H), 2.03 (br, 1H), 1.69−1.62 (m, 1H), 1.19 (br, 3H); ^{13}C NMR (100 MHz, $CDCl_3$) δ 158.0, 129.5, 114.3, 114.0, 109.0, 56.2, 55.5, 46.2, 32.1, 14.1; ESI-MS calcd for $C_{21}H_{29}NO_3^{2+}$ $[M + 2H]^+$ m/z 343.5, found m/z 343.5; HRMS (ESI) for $C_{21}H_{28}NO_3^+$ $[M + H]^+$ requires m/z 342.2069, found m/z 342.2065.

Synthesis of 7-Methoxy-2-{4-[4-(methoxymethoxy)phenyl]-butan-2-yl}-1,2,3,4-tetrahydroisoquinolin-6-ol [(±)-13]. A solution of (±)-**11** was synthesized via the same procedure that was used for (±)-**12** and purified by flash chromatography on silica gel (20:1 CH_2Cl_2/7 N NH_3 in MeOH) to afford (±)-**13** (12 mg, 50% yield) as a white solid: ^{1}H NMR (400 MHz, $CDCl_3$) δ 7.09 (d, J = 8.6 Hz, 2H), 6.93 (d, J = 8.6 Hz, 2H), 6.63 (s, 1H), 6.49 (s, 1H), 5.13 (s, 2H), 3.82 (s, 3H), 3.67 (d, J = 14 Hz, 1H), 3.56 (d, J = 14 Hz, 1H), 3.46 (s, 3H), 2.79−2.70 (m, 4H), 2.68−2.55 (m, 3H), 1.95−1.86 (m, 1H), 1.65−1.56 (m, 1H), 1.06 (d, J = 6.5 Hz, 3H); ^{13}C NMR (100 MHz, $CDCl_3$) δ 155.5, 145.0, 144.0, 136.3, 129.6, 127.7, 127.1, 116.4, 114.5, 109.1, 94.9, 58.1, 56.2, 56.1, 51.0, 46.1, 35.9, 32.4, 29.6, 14.0; ESI-MS calcd for $C_{21}H_{29}NO_3^{2+}$ $[M + 2H]^+$ m/z 373.5, found m/z 373.5; HRMS (ESI) for $C_{22}H_{30}NO_4^+$ $[M + H]^+$ requires m/z 372.2173, found m/z 372.2176.

Enantiomer Purification. (±)-7 was purified by a preparative chiral HPLC (stationary phase, Chiralpak AD-H, 30 mm × 250 mm, mobile phase of 20% methanol, including 0.1% DEA/80% CO_2, 100 bar, wavelength of 220 nm, flow rate of 70 mL/min), and two different fractions were collected corresponding to enantiomers (+)-7 and (−)-7. The purity of enantiomer (+)-7 or (−)-7 was measured by analytical HPLC [stationary phase, Chiralpak AD-H, 4.6 mm × 250 mm, mobile phase of 30% methanol, including 0.1% DEA/70% CO_2, 100 bar, wavelength of 220 nm, flow rate of 2 mL/min, retention times for (+)-7 of 5.0 min and for (−)-7 of 6.0 min]. The $[\alpha]_D^{25}$ for (+)-7 was +6.65 (c = 2.0, MeOH), and the $[\alpha]_D^{25}$ for (−)-7 was −5.94 (c = 2.0, MeOH). Enantiomers (+)-**8** and (−)-**8** were prepared using (±)-**8** under conditions more polar than those of (±)-7 (mobile phase of 30% methanol, including 0.1% DEA/70% CO_2), and the ee was measured under the same condition [retention times for (+)-**8** of 4.6 min and for (−)-**8** of 6.0 min]. The $[\alpha]_D^{25}$ for (+)-**8** was +7.33 (c = 2.0, MeOH), and the $[\alpha]_D^{25}$ for (−)-**8** was −7.26 (c = 2.0, MeOH).

Radiochemistry. All of the radiosyntheses for [^{11}C]-(±)-7 and [^{11}C]-(±)-**8** were performed in a Synthra MeIplus module using gas phase [^{11}C]CH_3I. First, [^{11}C]CO_2 was produced by using ^{14}N-(p,α)^{11}C and afforded the module. [^{11}C]CO_2 was trapped at −180 °C and reduced to [^{11}C]CH_4 on a Ni catalyst with hydrogen and a molecular sieve. Then, [^{11}C]CH_4 was converted to [^{11}C]CH_3I through an iodine column and trapped on Porapak Q for labeling.

To synthesize [^{11}C]-(±)-7, [^{11}C]CH_3I was bubbled into a solution of 1 mg of (±)-**12** and 2.4 μL of 5 N NaOH in 0.5 mL of DMF at −30 °C and the reaction mixture was heated at 70 °C for 5 min. The mixture was cooled to room temperature and added to 1 mL of the mobile phase. The crude mixture was purified using prepareative HPLC (stationary phase, Gemini 5 μm C18 100 Å, 10 mm × 250 mm, mobile phase of 70% pH 8.0 50 mM potassium phosphate buffer in MeCN, wavelength of 254 nm, flow rate of 5 mL/min, retention time of 10.8 min). [^{11}C]Methyl was introduced on (±)-**13** in the same manner as [^{11}C]-(±)-7. For MOM deprotection, 0.5 mL of 2 N aqueous HCl was added to the reaction mixture and the mixture was heated to 80 °C for 5 min. The mixture was cooled to room temperature, and 0.2 mL of 5 N NaOH and 0.8 mL of the mobile phase mixture were added. Purification was preformed using prepareative HPLC to afford [^{11}C]-(±)-**8** (stationary phase, Gemini 5 μm C18 100 Å, 10 mm × 250 mm, mobile phase of 55% pH 8.0 50 mM potassium phosphate buffer in MeCN, wavelength of 254 nm, flow rate of 3 mL/min, retention time of 12.3 min).

After purification, both compounds were formulated for the *in vivo* experiments. The collected product fraction was passed on a Sep-Pak *t*C18 cartridge and washed with 10 mL of water. The final product was eluted with 1 mL of ethanol and diluted with normal saline.

The radioactivity of the final solution was measured using a dose calibrator. The radiochemical purity was analyzed by HPLC prior to animal studies, and the molar activity was calculated on the basis of the amount of (±)-7 or (±)-**8** [stationary phase, Waters acquity UPLC BEH 1.7 μm C18 130 Å, 2.1 mm × 50 mm, mobile phase of 75% of 0.1% TFA in MeCN for [^{11}C]-(±)-7 and 82% of 0.1% TFA in MeCN for [^{11}C]-(±)-**8**, wavelength of 230 nm, flow rate of 0.5 mL/min, retention times of 2.7 min for [^{11}C]-(±)-7 and 2.5 min for [^{11}C]-(±)-**8**].

Distribution Coefficient (log $D_{7.4}$). The log $D_{7.4}$ values of [^{11}C]-(±)-7 and [^{11}C]-(±)-**8** were measured in an *n*-octanol/0.01 M phosphate buffer (pH 7.4) solution [1:2 (v/v)] by a shake-flask method. Each experiment was performed in quintuplicate, and log $D_{7.4}$ was calculated as the log value of the ratio of radioactivity in *n*-octanol to that in phosphate buffer.

***In Vitro* Cell Binding Assay.** PGRMC1 KO, TMEM97 KO, and DKO HeLa cells were prepared according to the described method.[48] Each cell membrane (100 μg) was incubated in the presence of 10 nM [^{11}C]-(±)-7 or [^{11}C]-(±)-**8** at 37 °C for 30 min. Nonspecific binding was assessed by incubation in the presence of 10 μM RHM-4. After incubation, bound ligands were collected using an M-24 Brandel filtration system (Brandel, Gaithersburg, MD) using GF-B filter papers and immediately counted using a Wizard2 Automatic Gamma Counter (2470). Specific binding was assessed by subtracting nonspecific binding from total binding, and specific binding in the knockout cell lines was normalized to control cell counts to determine the total percentage bound. All studies were performed three times in duplicate. GraphPad Prism version 9 (GraphPad, La Jolla, CA) was used to analyze the results using one-way analysis of variance (ANOVA); data represent means ± the standard deviation (n = 3; ****p < 0.0001).

PET Study. Female C57BL/6J mice (6−8 weeks of age), weighing 18.2 ± 0.8 g, were anesthetized with 2% (v/v) isoflurane at an oxygen flow of 1 L/min, and [^{11}C]-(±)-7 or [^{11}C]-(±)-**8** (9.9 ± 1.0 MBq) was injected through the tail vein. PET dynamic images were taken for 60 min using a Molecubes (MOLECUBES NV) PET instrument. For blocking PET, 1 mg of blocking agent [(±)-7, haloperidol, or siramesine] per kilogram was treated 10 min before [^{11}C]-(±)-7 or [^{11}C]-(±)-**8** injections. Micro-PET/CT images were analyzed by using Pmod software (version 3.7, PMOD Technologies Ltd., Zurich, Switzerland). Each micro-CT image was manually co-registered to the Mirrione T2 mouse brain template[57] by using rigid body transformation. Then, the resulting transformation parameters were applied to the corresponding micro-PET image. Fifteen volumes of interest (VOIs), including cortex, thalamus, cerebellum, basal forebrain septum, hypothalamus, brain stem, central gray, superior colliculi, olfactory bulb, striatum, hippocampus, amygdala, midbrain, inferior colliculi, and whole brain, were selected from the Mirrione atlas.[57] TACs were extracted from all of the VOIs and performed as the percentage injection dose per cubic centimeter (%ID/cc). The TAC of normalized to pick value was also calculated from whole brain VOI for washout rate evaluation.

Tissue Binding Study. Prepared homogenates (50 μg of cortex or thalamus) were mixed with 0.2 nM [^{11}C]-(±)-7 and 10 nM (±)-7, haloperidol, siramesine, or pentazocine. The mixture was incubated for 30 min at 37 °C and filtered through a Whatman CF/C filter in a harvester. The residue was washed using cold washing buffer (10 mM Tris-HCl and 150 mM NaCl). The residue was collected, and the radioactivity of each residue was counted with a γ counter. Two-way ANOVA was performed using PRISM 8 software (**p < 0.001, ***p < 0.0005, and ****p < 0.0001).

https://doi.org/10.1021/acs.jmedchem.2c00191
J. Med. Chem. 2022, 65, 6261−6272

Metabolite Study. [^{11}C]-(±)-7 (19.6 ± 1.2 MBq; n = 4) was injected and sacrificed after 30 min. Brain and blood were obtained immediately and stored on ice. Obtained brain was mixed with MeCN and homogenized using a pellet pestle for a few seconds. Brain homogenate was centrifuged at 20000g for 10 min at 4 °C. After the supernatant had been collected, the pellet was resuspended upon addition of ice-cold HPLC buffer (65% pH 8.0 50 mM potassium phosphate buffer in MeCN) and recentrifuged at 20000g for 10 min. Two supernatants were mixed and filtered for HPLC injection. For the plasma sample, ethanol was added to the collected blood and vortexed for a few seconds, followed by centrifugation at 500g for 10 min at 4 °C. The supernatant was collected, and the pellet was resuspended using ice-cold buffer for another centrifugation (500g for 10 min at 4 °C). The collected supernatant was mixed and stored on ice for HPLC.

The metabolites from the brain or plasma were injected into the HPLC system (stationary phase, Gemini 5 μm C18 100 Å, 250 mm × 10 mm, mobile phase of 65% pH 8.0 50 mM potassium phosphate buffer in MeCN, flow rate of 3 mL/min), and the eluate was collected for 30 s. The radioactivity of the collected fractions was measured with a γ counter [retention times of metabolite of 4.5 min and [^{11}C]-(±)-7 of 17.0 min].

■ ASSOCIATED CONTENT

Supporting Information

The Supporting Information is available free of charge at https://pubs.acs.org/doi/10.1021/acs.jmedchem.2c00191.

Structures, purities, and *in vitro* binding assay results of screened compounds, chiral analytical HPLC chromatograms for (+)-7 and (−)-7 or (+)-8 and (−)-8, preparative and analytical HPLC chromatograms for [^{11}C]-(±)-7 and [^{11}C]-(±)-8, metabolite profile of [^{11}C]-(±)-7, and ^{1}H and ^{13}C NMR spectra of compounds (±)-7, (±)-8, **10**−**13**, and **9** (PDF)

Molecular formula strings (CSV)

■ AUTHOR INFORMATION

Corresponding Author

Robert H. Mach − *Department of Radiology, University of Pennsylvania, Philadelphia, Pennsylvania 19104-6323, United States;* orcid.org/0000-0002-7645-2869; Email: rmach@pennmedicine.upenn.edu

Authors

Ho Young Kim − *Department of Radiology, University of Pennsylvania, Philadelphia, Pennsylvania 19104-6323, United States;* orcid.org/0000-0003-4391-9642

Ji Youn Lee − *Department of Radiology, University of Pennsylvania, Philadelphia, Pennsylvania 19104-6323, United States*

Chia-Ju Hsieh − *Department of Radiology, University of Pennsylvania, Philadelphia, Pennsylvania 19104-6323, United States;* orcid.org/0000-0002-2833-7727

Aladdin Riad − *Department of Radiology, University of Pennsylvania, Philadelphia, Pennsylvania 19104-6323, United States;* orcid.org/0000-0002-0525-446X

Nicholas J. Izzo − *Cognition Therapeutics Inc., Pittsburgh, Pennsylvania 15203-5118, United States;* orcid.org/0000-0002-0196-2055

Susan M. Catalano − *Cognition Therapeutics Inc., Pittsburgh, Pennsylvania 15203-5118, United States*

Thomas J. A. Graham − *Department of Radiology, University of Pennsylvania, Philadelphia, Pennsylvania 19104-6323, United States*

Complete contact information is available at: https://pubs.acs.org/10.1021/acs.jmedchem.2c00191

Notes

The authors declare no competing financial interest.

■ ACKNOWLEDGMENTS

We thank the following funding agent for their generous support of this work: National Institutes of Health, Grant R42AG052249.

■ ABBREVIATIONS USED

Aβ, amyloid β-protein; ApoE, apolipoprotein E; DIPEA, *N*,*N*-diisopropylethylamine; LDL, low-density lipoprotein; MOMCl, methoxymethyl chloride; PET, positron emission tomography; PGRMC1, progesterone receptor membrane component 1

■ REFERENCES

(1) Martin, W. R.; Eades, C. G.; Thompson, J. A.; Huppler, R. E.; Gilbert, P. E. The effects of morphine- and nalorphine- like drugs in the nondependent and morphine-dependent chronic spinal dog. *J. Pharmacol. Exp. Ther.* **1976**, *197*, 517−532.

(2) Khazan, N.; Young, G. A.; El-Fakany, E. E.; Hong, O.; Calligaro, D. Sigma receptors mediated the psychotomimetic effects of N-allylnormetazocine (SKF-10,047), but not its opioid agonistic-antagonistic properties. *Neuropharmacology* **1984**, *23*, 983−987.

(3) Hellewell, S. B.; Bowen, W. D. A sigma-like binding site in rat pheochromocytoma (PC12) cells: decreased affinity for (+)-benzomorphans and lower molecular weight suggest a different sigma receptor form from that of guinea pig brain. *Brain Res.* **1990**, *527*, 244−253.

(4) Pal, A.; Hajipour, A. R.; Fontanilla, D.; Ramachandran, S.; Chu, U. B.; Mavlyutov, T.; Ruoho, A. E. Identification of regions of the sigma-1 receptor ligand binding site using a novel photoprobe. *Mol. Pharmacol.* **2007**, *72*, 921−933.

(5) Bouchard, P.; Quirion, R. [3H]1,3-di(2-tolyl)guanidine and [3H](+)pentazocine binding sites in the rat brain: autoradiographic visualization of the putative sigma1 and sigma2 receptor subtypes. *Neuroscience* **1997**, *76*, 467−477.

(6) Hellewell, S. B.; Bruce, A.; Feinstein, G.; Orringer, J.; Williams, W.; Bowen, W. D. Rat liver and kidney contain high densities of sigma 1 and sigma 2 receptors: characterization by ligand binding and photoaffinity labeling. *Eur. J. Pharmacol.* **1994**, *268*, 9−18.

(7) Quirion, R.; Bowen, W. D.; Itzhak, Y.; Junien, J. L.; Musacchio, J. M.; Rothman, R. B.; Tsung-Ping, S.; Tam, S. W.; Taylor, D. P. A proposal for the classification of sigma binding sites. *Trends Pharmacol. Sci.* **1992**, *13*, 85−86.

(8) Alon, A.; Schmidt, H. R.; Wood, M. D.; Sahn, J. J.; Martin, S. F.; Kruse, A. C. Identification of the gene that codes for the sigma2 receptor. *Proc. Natl. Acad. Sci. U. S. A.* **2017**, *114*, 7160−7165.

(9) Mach, R. H.; Smith, C. R.; Al-Nabulsi, I.; Whirrett, B. R.; Childers, S. R.; Wheeler, K. T. Sigma 2 receptors as potential biomarkers of proliferation in breast cancer. *Cancer Res.* **1997**, *57*, 156−161.

(10) Wheeler, K. T.; Wang, L. M.; Wallen, C. A.; Childers, S. R.; Cline, J. M.; Keng, P. C.; Mach, R. H. Sigma-2 receptors as a biomarker of proliferation in solid tumours. *Br. J. Cancer* **2000**, *82*, 1223−1232.

(11) Zhang, H.; Cuevas, J. Sigma receptors inhibit high-voltage-activated calcium channels in rat sympathetic and parasympathetic neurons. *J. Neurophysiol* **2002**, *87*, 2867−2879.

(12) Garces-Ramirez, L.; Green, J. L.; Hiranita, T.; Kopajtic, T. A.; Mereu, M.; Thomas, A. M.; Mesangeau, C.; Narayanan, S.; McCurdy, C. R.; Katz, J. L.; Tanda, G. Sigma receptor agonists: receptor binding and effects on mesolimbic dopamine neurotransmission assessed by microdialysis. *Biol. Psychiatry* **2011**, *69*, 208−217.

(13) Nuwayhid, S. J.; Werling, L. L. Sigma2 (sigma2) receptors as a target for cocaine action in the rat striatum. *Eur. J. Pharmacol.* **2006**, *535*, 98−103.
(14) Scott, L. L.; Sahn, J. J.; Ferragud, A.; Yen, R. C.; Satarasinghe, P. N.; Wood, M. D.; Hodges, T. R.; Shi, T.; Prakash, B. A.; Friese, K. M.; Shen, A.; Sabino, V.; Pierce, J. T.; Martin, S. F. Small molecule modulators of sigma2R/Tmem97 reduce alcohol withdrawal-induced behaviors. *Neuropsychopharmacology* **2018**, *43*, 1867−1875.
(15) Yi, B.; Sahn, J. J.; Ardestani, P. M.; Evans, A. K.; Scott, L. L.; Chan, J. Z.; Iyer, S.; Crisp, A.; Zuniga, G.; Pierce, J. T.; Martin, S. F.; Shamloo, M. Small molecule modulator of sigma 2 receptor is neuroprotective and reduces cognitive deficits and neuroinflammation in experimental models of Alzheimer's disease. *J. Neurochem* **2017**, *140*, 561−575.
(16) Terada, K.; Migita, K.; Matsushima, Y.; Sugimoto, Y.; Kamei, C.; Matsumoto, T.; Mori, M.; Matsunaga, K.; Takata, J.; Karube, Y. Cholinesterase inhibitor rivastigmine enhances nerve growth factor-induced neurite outgrowth in PC12 cells via sigma-1 and sigma-2 receptors. *PLoS One* **2018**, *13*, No. e0209250.
(17) Vazquez-Rosa, E.; Watson, M. R.; Sahn, J. J.; Hodges, T. R.; Schroeder, R. E.; Cintron-Perez, C. J.; Shin, M. K.; Yin, T. C.; Emery, J. L.; Martin, S. F.; Liebl, D. J.; Pieper, A. A. Neuroprotective efficacy of a sigma 2 receptor/TMEM97 modulator (DKR-1677) after traumatic brain injury. *ACS Chem. Neurosci.* **2019**, *10*, 1595−1602.
(18) Helmeste, D. M.; Tang, S. W.; Bunney, W. E., Jr; Potkin, S. G.; Jones, E. G. Decrease in sigma but no increase in striatal dopamine D4 sites in schizophrenic brains. *Eur. J. Pharmacol.* **1996**, *314*, R3−5.
(19) Sanchez, C.; Arnt, J.; Costall, B.; Kelly, M. E.; Meier, E.; Naylor, R. J.; Perregaard, J. The selective sigma2-ligand Lu 28−179 has potent anxiolytic-like effects in rodents. *J. Pharmacol. Exp. Ther.* **1997**, *283*, 1323−1332.
(20) Sanchez, C.; Papp, M. The selective sigma2 ligand Lu 28−179 has an antidepressant-like profile in the rat chronic mild stress model of depression. *Behav Pharmacol* **2000**, *11*, 117−124.
(21) Riad, A.; Lengyel-Zhand, Z.; Zeng, C.; Weng, C. C.; Lee, V. M.; Trojanowski, J. Q.; Mach, R. H. The sigma-2 receptor/TMEM97, PGRMC1, and LDL receptor complex are responsible for the cellular uptake of Abeta42 and its protein aggregates. *Mol. Neurobiol* **2020**, *57*, 3803−3813.
(22) Mach, R. H.; Huang, Y.; Freeman, R. A.; Wu, L.; Vangveravong, S.; Luedtke, R. R. Conformationally-flexible benzamide analogues as dopamine D3 and sigma 2 receptor ligands. *Bioorg. Med. Chem. Lett.* **2004**, *14*, 195−202.
(23) Tu, Z.; Xu, J.; Jones, L. A.; Li, S.; Dumstorff, C.; Vangveravong, S.; Chen, D. L.; Wheeler, K. T.; Welch, M. J.; Mach, R. H. Fluorine-18-labeled benzamide analogues for imaging the sigma2 receptor status of solid tumors with positron emission tomography. *J. Med. Chem.* **2007**, *50*, 3194−3204.
(24) Zeng, C.; Rothfuss, J. M.; Zhang, J.; Vangveravong, S.; Chu, W.; Li, S.; Tu, Z.; Xu, J.; Mach, R. H. Functional assays to define agonists and antagonists of the sigma-2 receptor. *Anal. Biochem.* **2014**, *448*, 68−74.
(25) Dehdashti, F.; Laforest, R.; Gao, F.; Shoghi, K. I.; Aft, R. L.; Nussenbaum, B.; Kreisel, F. H.; Bartlett, N. L.; Cashen, A.; Wagner-Johnson, N.; Mach, R. H. Assessment of cellular proliferation in tumors by PET using 18F-ISO-1. *J. Nucl. Med.* **2013**, *54*, 350−357.
(26) Tu, Z.; Xu, J.; Jones, L. A.; Li, S.; Zeng, D.; Kung, M. P.; Kung, H. F.; Mach, R. H. Radiosynthesis and biological evaluation of a promising sigma(2)-receptor ligand radiolabeled with fluorine-18 or iodine-125 as a PET/SPECT probe for imaging breast cancer. *Appl. Radiat. Isot.* **2010**, *68*, 2268−2273.
(27) Shoghi, K. I.; Xu, J.; Su, Y.; He, J.; Rowland, D.; Yan, Y.; Garbow, J. R.; Tu, Z.; Jones, L. A.; Higashikubo, R.; Wheeler, K. T.; Lubet, R. A.; Mach, R. H.; You, M. Quantitative receptor-based imaging of tumor proliferation with the sigma-2 ligand [(18)F]ISO-1. *PLoS One* **2013**, *8*, No. e74188.
(28) Intagliata, S.; Sharma, A.; King, T. I.; Mesangeau, C.; Seminerio, M.; Chin, F. T.; Wilson, L. L.; Matsumoto, R. R.; McLaughlin, J. P.; Avery, B. A.; McCurdy, C. R. Discovery of a highly selective sigma-2 receptor ligand, 1-(4-(6,7-dimethoxy-3,4-dihydroisoquinolin-2(1H)-yl)butyl)-3-methyl-1H-benzo[d]imidazol-2(3H)-one (CM398), with drug-like properties and antinociceptive effects in vivo. *AAPS J.* **2020**, *22*, 94.
(29) Mesangeau, C.; Narayanan, S.; Green, A. M.; Shaikh, J.; Kaushal, N.; Viard, E.; Xu, Y. T.; Fishback, J. A.; Poupaert, J. H.; Matsumoto, R. R.; McCurdy, C. R. Conversion of a highly selective sigma-1 receptor-ligand to sigma-2 receptor preferring ligands with anticocaine activity. *J. Med. Chem.* **2008**, *51*, 1482−1486.
(30) Zampieri, D.; Grazia Mamolo, M.; Laurini, E.; Zanette, C.; Florio, C.; Collina, S.; Rossi, D.; Azzolina, O.; Vio, L. Substituted benzo[d]oxazol-2(3H)-one derivatives with preference for the sigma1 binding site. *Eur. J. Med. Chem.* **2009**, *44*, 124−130.
(31) Kaushal, N.; Robson, M. J.; Vinnakota, H.; Narayanan, S.; Avery, B. A.; McCurdy, C. R.; Matsumoto, R. R. Synthesis and pharmacological evaluation of 6-acetyl-3-(4-(4-(4-fluorophenyl)-piperazin-1-yl)butyl)benzo[d]oxazol-2(3H)-one (SN79), a cocaine antagonist, in rodents. *AAPS J.* **2011**, *13*, 336−346.
(32) Xu, Y. T.; Kaushal, N.; Shaikh, J.; Wilson, L. L.; Mesangeau, C.; McCurdy, C. R.; Matsumoto, R. R. A novel substituted piperazine, CM156, attenuates the stimulant and toxic effects of cocaine in mice. *J. Pharmacol Exp Ther* **2010**, *333*, 491−500.
(33) Laurini, E.; Zampieri, D.; Mamolo, M. G.; Vio, L.; Zanette, C.; Florio, C.; Posocco, P.; Fermeglia, M.; Pricl, S. A 3D-pharmacophore model for sigma2 receptors based on a series of substituted benzo[d]oxazol-2(3H)-one derivatives. *Bioorg. Med. Chem. Lett.* **2010**, *20*, 2954−2957.
(34) Romeo, G.; Prezzavento, O.; Intagliata, S.; Pittala, V.; Modica, M. N.; Marrazzo, A.; Turnaturi, R.; Parenti, C.; Chiechio, S.; Arena, E.; Campisi, A.; Sposito, G.; Salerno, L. Synthesis, in vitro and in vivo characterization of new benzoxazole and benzothiazole-based sigma receptor ligands. *Eur. J. Med. Chem.* **2019**, *174*, 226−235.
(35) Bonhaus, D. W.; Loury, D. N.; Jakeman, L. B.; To, Z.; DeSouza, A.; Eglen, R. M.; Wong, E. H. [3H]BIMU-1, a 5-hydroxytryptamine3 receptor ligand in NG-108 cells, selectively labels sigma-2 binding sites in guinea pig hippocampus. *J. Pharmacol. Exp. Ther.* **1993**, *267*, 961−970.
(36) Intagliata, S.; Alsharif, W. F.; Mesangeau, C.; Fazio, N.; Seminerio, M.; Xu, Y. T.; Matsumoto, R. R.; McCurdy, C. R. Benzimidazolone-based selective sigma2 receptor ligands: Synthesis and pharmacological evaluation. *Eur. J. Med. Chem.* **2019**, *165*, 250−257.
(37) Izzo, N. J.; Staniszewski, A.; To, L.; Fa, M.; Teich, A. F.; Saeed, F.; Wostein, H.; Walko, T., 3rd; Vaswani, A.; Wardius, M.; Syed, Z.; Ravenscroft, J.; Mozzoni, K.; Silky, C.; Rehak, C.; Yurko, R.; Finn, P.; Look, G.; Rishton, G.; Safferstein, H.; Miller, M.; Johanson, C.; Stopa, E.; Windisch, M.; Hutter-Paier, B.; Shamloo, M.; Arancio, O.; LeVine, H., 3rd; Catalano, S. M. Alzheimer's therapeutics targeting amyloid beta 1−42 oligomers I: Abeta 42 oligomer binding to specific neuronal receptors is displaced by drug candidates that improve cognitive deficits. *PLoS One* **2014**, *9*, No. e111898.
(38) Grundman, M.; Morgan, R.; Lickliter, J. D.; Schneider, L. S.; DeKosky, S.; Izzo, N. J.; Guttendorf, R.; Higgin, M.; Pribyl, J.; Mozzoni, K.; Safferstein, H.; Catalano, S. M. A phase 1 clinical trial of the sigma-2 receptor complex allosteric antagonist CT1812, a novel therapeutic candidate for Alzheimer's disease. *Alzheimers Dement (N Y)* **2019**, *5*, 20−26.
(39) Izzo, N. J.; Yuede, C. M.; LaBarbera, K. M.; Limegrover, C. S.; Rehak, C.; Yurko, R.; Waybright, L.; Look, G.; Rishton, G.; Safferstein, H.; Hamby, M. E.; Williams, C.; Sadlek, K.; Edwards, H. M.; Davis, C. S.; Grundman, M.; Schneider, L. S.; DeKosky, S. T.; Chelsky, D.; Pike, I.; Henstridge, C.; Blennow, K.; Zetterberg, H.; LeVine, H., 3rd; Spires-Jones, T. L.; Cirrito, J. R.; Catalano, S. M. Preclinical and clinical biomarker studies of CT1812: A novel approach to Alzheimer's disease modification. *Alzheimers Dement* **2021**, *17*, 1365−1382.
(40) Moldovan, R. P.; Gundel, D.; Teodoro, R.; Ludwig, F. A.; Fischer, S.; Toussaint, M.; Schepmann, D.; Wunsch, B.; Brust, P.; Deuther-Conrad, W. Design, radiosynthesis and preliminary biological

https://doi.org/10.1021/acs.jmedchem.2c00191
J. Med. Chem. 2022, 65, 6261−6272

evaluation in mice of a brain-penetrant (18)F-labelled sigma2 receptor ligand. *Int. J. Mol. Sci.* **2021**, *22*, 5447.
(41) Zhang, Y.; Wang, T.; Zhang, X.; Deuther-Conrad, W.; Fu, H.; Cui, M.; Zhang, J.; Brust, P.; Huang, Y.; Jia, H. Discovery and development of brain-penetrant 18F-labeled radioligands for neuroimaging of the sigma-2 receptors. *Acta Pharmaceutica Sinica B* **2022**, *12*, 1406.
(42) Abate, C.; Selivanova, S. V.; Müller, A.; Krämer, S. D.; Schibli, R.; Marottoli, R.; Perrone, R.; Berardi, F.; Niso, M.; Ametamey, S. M. Development of 3,4-dihydroisoquinolin-1(2H)-one derivatives for the Positron Emission Tomography (PET) imaging of σ receptors. *Eur. J. Med. Chem.* **2013**, *69*, 920−930.
(43) Alon, A.; Lyu, J.; Braz, J. M.; Tummino, T. A.; Craik, V.; O'Meara, M. J.; Webb, C. M.; Radchenko, D. S.; Moroz, Y. S.; Huang, X. P.; Liu, Y.; Roth, B. L.; Irwin, J. J.; Basbaum, A. I.; Shoichet, B. K.; Kruse, A. C. Structures of the sigma2 receptor enable docking for bioactive ligand discovery. *Nature* **2021**, *600*, 759−764.
(44) Mach, R. H.; Zeng, C.; Hawkins, W. G. The sigma2 receptor: a novel protein for the imaging and treatment of cancer. *J. Med. Chem.* **2013**, *56*, 7137−7160.
(45) Ablordeppey, S. Y.; Fischer, J. B.; Glennon, R. A. Is a nitrogen atom an important pharmacophoric element in sigma ligand binding? *Bioorg. Med. Chem.* **2000**, *8*, 2105−2111.
(46) Mach, R. H.; Smith, C. R.; Childers, S. R. Ibogaine possesses a selective affinity for sigma 2 receptors. *Life Sci.* **1995**, *57*, PL57−62.
(47) Xu, J.; Zeng, C.; Chu, W.; Pan, F.; Rothfuss, J. M.; Zhang, F.; Tu, Z.; Zhou, D.; Zeng, D.; Vangveravong, S.; Johnston, F.; Spitzer, D.; Chang, K. C.; Hotchkiss, R. S.; Hawkins, W. G.; Wheeler, K. T.; Mach, R. H. Identification of the PGRMC1 protein complex as the putative sigma-2 receptor binding site. *Nat. Commun.* **2011**, *2*, 380.
(48) Riad, A.; Zeng, C.; Weng, C. C.; Winters, H.; Xu, K.; Makvandi, M.; Metz, T.; Carlin, S.; Mach, R. H. Sigma-2 receptor/TMEM97 and PGRMC-1 increase the rate of internalization of LDL by LDL receptor through the formation of a ternary complex. *Sci. Rep.* **2018**, *8*, 16845.
(49) Wager, T. T.; Hou, X.; Verhoest, P. R.; Villalobos, A. Moving beyond rules: the development of a central nervous system multiparameter optimization (CNS MPO) approach to enable alignment of druglike properties. *ACS Chem. Neurosci.* **2010**, *1*, 435−449.
(50) Xie, X. Y.; Li, Y. Y.; Ma, W. H.; Chen, A. F.; Sun, Y. T.; Lee, J. Y.; Riad, A.; Xu, D. H.; Mach, R. H.; Huang, Y. S. Synthesis, binding, and functional properties of tetrahydroisoquinolino-2-alkyl phenones as selective sigma2R/TMEM97 ligands. *Eur. J. Med. Chem.* **2021**, *209*, 112906.
(51) Leese, M. P.; Jourdan, F. L.; Major, M. R.; Dohle, W.; Hamel, E.; Ferrandis, E.; Fiore, A.; Kasprzyk, P. G.; Potter, B. V. Tetrahydroisoquinolinone-based steroidomimetic and chimeric microtubule disruptors. *ChemMedChem.* **2014**, *9*, 85−108.
(52) Di, L.; Kerns, E. H. Profiling drug-like properties in discovery research. *Curr. Opin Chem. Biol.* **2003**, *7*, 402−8.
(53) Vangveravong, S.; Xu, J.; Zeng, C.; Mach, R. H. Synthesis of N-substituted 9-azabicyclo[3.3.1]nonan-3alpha-yl carbamate analogs as sigma2 receptor ligands. *Bioorg. Med. Chem.* **2006**, *14*, 6988−6897.
(54) Abatematteo, F. S.; Niso, M.; Lacivita, E.; Abate, C. Sigma2 receptor and its role in cancer with focus on a multitarget directed ligand (MTDL) approach. *Molecules* **2021**, *26*, 3743.
(55) Rishton, G. M.; Look, G. C.; Ni, Z. J.; Zhang, J.; Wang, Y.; Huang, Y.; Wu, X.; Izzo, N. J.; LaBarbera, K. M.; Limegrover, C. S.; Rehak, C.; Yurko, R.; Catalano, S. M. Discovery of investigational drug CT1812, an antagonist of the sigma-2 receptor complex for alzheimer's disease. *ACS Med. Chem. Lett.* **2021**, *12*, 1389−1395.
(56) Ferrie, J. J.; Lengyel-Zhand, Z.; Janssen, B.; Lougee, M. G.; Giannakoulias, S.; Hsieh, C. J.; Pagar, V. V.; Weng, C. C.; Xu, H.; Graham, T. J. A.; Lee, V. M.; Mach, R. H.; Petersson, E. J. Identification of a nanomolar affinity alpha-synuclein fibril imaging probe by ultra-high throughput in silico screening. *Chem. Sci.* **2020**, *11*, 12746−12754.
(57) Mirrione, M. M.; Schiffer, W. K.; Fowler, J. S.; Alexoff, D. L.; Dewey, S. L.; Tsirka, S. E. A novel approach for imaging brain-behavior relationships in mice reveals unexpected metabolic patterns during seizures in the absence of tissue plasminogen activator. *Neuroimage* **2007**, *38*, 34−42.

NOTE ADDED AFTER ASAP PUBLICATION

Due to a production error, this article published with incorrect Scheme 1 and 2 files. The correct schemes published April 18, 2022.

https://doi.org/10.1021/acs.jmedchem.2c00191
J. Med. Chem. 2022, 65, 6261−6272